Thermochimica Acta 498 (2010) 71–80

Contents lists available at ScienceDirect

Thermochimica Acta

journal homepage: www.elsevier.com/locate/tca

Kinetic analysis of thermal degradation of poly(ethylene glycol) and poly(ethylene oxide)s of different molecular weight

Nataša Stipanelov Vrandečić, Matko Erceg*, Miće Jakić, Ivka Klarić

Department of Organic Technology, Faculty of Chemistry and Technology, University of Split, Teslina 10/V, HR-21000 Split, Croatia

ARTICLE INFO

Article history:
Received 24 August 2009
Received in revised form 2 October 2009
Accepted 4 October 2009
Available online 13 October 2009

Keywords:
Differential scanning calorimetry
Dynamic thermogravimetry
Fourier transform-infra red spectroscopy
Kinetic analysis
Poly(ethylene glycol)
Poly(ethylene oxide)

ABSTRACT

The effect of molecular weight on thermal characteristics and thermal degradation of poly(ethylene glycol) (PEG) and poly(ethylene oxide)s (PEO) was investigated by differential scanning calorimetry, FT-IR spectroscopy and dynamic thermogravimetry. Kinetic analysis of the non-isothermal degradation was performed using isoconversional (Flynn–Wall–Ozawa, Kissinger–Akahira–Sunose and Friedman) and the invariant kinetic parameters method. The empirical kinetic triplets (E, A, and $f(\alpha)$) as well as the rate constants have been calculated. The relation between the heating rate, the degradation rate and molecular weight for all investigated samples has been established.

1. Introduction

Poly(ethylene glycol) (PEG) and poly(ethylene oxide) (PEO) are the most commercially important polyethers. PEG refers to an oligomer (molecular weight below 20,000) and PEO is polymer of ethylene oxide commercially available in the wide range of molecular weights (20,000–8,000,000) [1]. Besides the differences in molecular weight PEG and PEOs have different end groups; PEG has –OH and PEOs have $-CH_3$ end group. PEO is semi-crystalline, biocompatible, biodegradable, non-ionic and water-soluble polymer of considerable industrial significance which finds applications in many different branches of industry [2]. Although PEG and PEO are used in different applications and have different physical properties (e.g. viscosity) due to chain length effects, their chemical properties are nearly identical. PEG is a component of many pharmaceutical and cosmetical products. PEO is currently also used in the pharmaceutical industry in applications such as controlled-release, solid-dose matrix systems, transdermal drug delivery systems and mucosal bioadhesives [3]. In recent time hot melt extrusion, process commonly used in plastic industry, is becoming accepted for preparation of some kinds of pharmaceutical products. Based on knowledge from the plastic industry, formulators extrude combinations of drugs, polymers and plasticizers into various final forms to achieve desired drug-release profiles. PEO is a very suitable material for hot melt extrusion due to its very good processability in different processing conditions, where polymer of low molecular weight can act as a plasticizer for high molecular weight polymer. Crowley et al. [3] have used PEO of molecular weight 100,000 as plasticizer for PEO 1,000,000 and found out that low molecular weight PEO degrades more rapidly than higher molecular weight one. Since hot melt extrusion exposes polymer to elevated temperatures, a good knowledge of thermal characteristics and stability of the material is very important.

The results of the non-isothermal thermogravimetry (TG) are often used for determination of thermal stability of polymers and kinetic analysis. Kinetic analysis aims to calculate kinetic parameters of the investigated process, i.e. the activation energy (E), the pre-exponential factor (A) and kinetic model ($f(\alpha)$), the so-called "kinetic triplet". Kinetic analysis of the non-isothermal degradation of PEG and PEO of different molecular weights has already been studied. Wang et al. [4] have calculated E values for PEO of $M_w = 20{,}000$ by isoconversional Ozawa method [5] as $266.4 \pm 4.3\ \mathrm{kJ\,mol^{-1}}$, but not the kinetic model, $f(\alpha)$. Pielichowski and Flejtuch [2] have used isoconversional Flynn–Wall–Ozawa method [5,6] and found an increasing dependence of E on conversion, α in the whole conversion range. By applying the non-linear regression method and F-test they have concluded that R3 kinetic model gives the best fit of the non-isothermal degradation of PEO. Audebert and Aubineau [7] have obtained E value of $200\ \mathrm{kJ\,mol^{-1}}$ for PEO of $M_w = 27{,}000$ by using Flynn–Wall–Ozawa method. Calahorra et al. [8] have obtained E value $129\ \mathrm{kJ\,mol^{-1}}$ assuming F1 kinetic model for PEO of $M_w = 365{,}000$. Barbadillo et al. [9] have

* Corresponding author. Fax: +385 21 329 461.
E-mail address: merceg@ktf-split.hr (M. Erceg).

0040-6031/$ – see front matter © 2009 Elsevier B.V. All rights reserved.
doi:10.1016/j.tca.2009.10.005

found that the reaction order models are not applicable for kinetic description of the non-isothermal degradation of PEGs of M_w from 1500 to 3000. These results for the non-isothermal degradation of PEG and different molecular weight PEOs are inconsistent and meaningful kinetic conclusion concerning cannot be drawn. One of the major goals of this article is to calculate the true kinetic triplets of the non-isothermal degradation of different molecular weight PEOs. For this purpose, isoconversional Flynn–Wall–Ozawa (FWO), Kissinger–Akahira–Sunose (KAS) [10,11] and Friedman (FR) [12] methods in combination with the invariant kinetic parameters (IKP) method [13] and Pérez-Maqueda criterion [14] were used in accordance with the algorithm suggested by Budrugeac [15].

2. Experimental

2.1. Materials

The powders of PEG and PEO with different viscometric average molecular weights (M_v) as follows: PEG (3400), PEO 1 (1×10^5), PEO 3 (3×10^5), PEO 10 (1×10^6), PEO 50 (5×10^6) were purchased from Sigma–Aldrich.

2.2. Differential scanning calorimetry

The thermal characteristics of PEG and PEO were investigated by means of the differential scanning calorimetry (Mettler Toledo DSC 823^e), in the nitrogen atmosphere (50 cm^3 min^{-1}). The calibration was performed with metallic indium. The samples of approximately 25 mg were pressed in aluminium pans. For determination of glass transition temperature (T_g) the samples were heated at a rate of 20 °C min^{-1} from −90 to 120 °C, cooled at the same rate to −90 °C and reheated to 120 °C. The samples were kept at −90 and 120 °C for 10 min. The T_g was determined from second heating cycle as the onset temperature, $T_{g(onset)}$, and as the temperature at which the change of the specific heat capacity is equal to the half of its maximal value, $T_{g(midpoint)}$.

The melting point of polymers was determined from DSC curves obtained at the heating rate of 10 °C min^{-1} from 25 to 120 °C, as the onset temperature $T_{m(onset)}$, and as the temperature in the endotherm peak, $T_{m(max)}$.

2.3. FT-IR spectroscopy

FT-IR spectra of investigated polymers were recorded on PerkinElmer Spectrum One FT-IR spectrometer by the Horizontal Attenuated Total Reflectance (HATR) technique. The internal reflection crystal, made of zinc selenide, had a 45° angle of incidence to the IR beam. Spectra were acquired in the measurement range 4000–450 cm^{-1} at the room temperature. Signals were collected in 10 scans at a resolution of 4 cm^{-1} and were rationed against a background spectrum recorded from the clean, empty cell at 25 °C.

2.4. Dynamic thermogravimetry

The thermal degradation of PEG and PEOs was investigated by using PerkinElmer Pyris 1 TGA thermobalance. The studies were carried out in nitrogen flow (30 cm^3 min^{-1}) at the heating rates of 2.5, 5 and 10 °C min^{-1} in the temperature range 50–500 °C.

To evaluate the thermal stability of the investigated polymers different criteria can be used. From TG and DTG curves the following characteristics were determined: the temperature at 5% mass loss ($T_{5\%}$), the temperature at the maximal rate of degradation (T_{max}), the maximum rate of degradation (R_{max}), the conversion at the maximum rate of degradation (α_{max}) and the final mass loss (m_f).

3. Kinetic analysis

The non-isothermal TG data can be used for the kinetic analysis of the investigated process. Kinetic analysis of the solid-state reactions that are ruled by a single process is based on Eq. (1):

$$\frac{d\alpha}{dt} \cong \beta\frac{d\alpha}{dT} = A \cdot \exp\left(-\frac{E}{RT}\right) \cdot f(\alpha) \quad (1)$$

where α is the degree of conversion, β is the linear heating rate (°C min^{-1}), T is the absolute temperature (K), R is the general gas constant (J mol^{-1} K^{-1}) and t is the time (min). It is suggested that prior to any kinetic analysis one should investigate the complexity of the process by determining the dependence of E on α by isoconversional methods [16]. Namely, this dependence is considered as reliable criterion of the process complexity [16] and isoconversional methods are considered as the most reliable methods for the calculation of E and E vs. α dependence of thermally activated reactions [16,17]. If E does not depend on α, the investigated process is simple (overall single-stage) and can be described by unique kinetic triplet. Otherwise, the process is complex and the shape of the E vs. α curve indicates the possible reaction mechanism [16,17]. Therefore, E values and E vs. α dependence have been calculated by means of isoconversional method which can determine them without knowledge or assumption of kinetic model (model-free). On the other hand, they do not give any information about A and $f(\alpha)$. Hence, in this article the kinetic analysis is performed according to algorithm proposed by Budrugeac [15]. The application of this algorithm begins with isoconversional methods in order to establish the dependence of E on α. It was shown that in cases when E does not depend on α, the IKP method associated with the criterion of the independence of kinetic parameters on the heating rate (Pérez-Maqueda et al. criterion) is recommended for evaluation of the kinetic triplet without any assumptions concerning kinetic model [15].

Table 1
Algebraic expressions for $f(\alpha)$ and $g(\alpha)$ for the most frequently used mechanisms [20,21].

Mechanism	Symbol	$f(\alpha)$	$g(\alpha)$
Reaction order model	Fn[a]	$(1-\alpha)^m$	$-\ln(1-\alpha)$, for $n=1$ $(1-(1-\alpha)^{(-n+1)})/(-n+1)$, for $n \neq 1$
Random nucleation and growth of nuclei (Avrami-Erofeev eq.)	Am[b] ($0.5 \leq m \leq 4$)	$m(1-\alpha)[-\ln(1-\alpha)]^{(1-1/m)}$	$[-\ln(1-\alpha)]^{1/m}$
1D diffusion (parabolic law)	D1	$1/2\alpha$	α^2
1D diffusion (bidimensional particle shape)	D2	$1/[-\ln(1-\alpha)]$	$(1-\alpha)\ln(1-\alpha)+\alpha$
1D diffusion (tridimensional particle shape) (Jander eq.)	D3	$(3(1-\alpha)^{2/3})/(2[1-(1-\alpha)^{1/3}])$	$[1-(1-\alpha)^{1/3}]^2$
1D diffusion (tridimensional particle shape) (GinstlingBrounshtein eq.)	D4	$3/(2[(1-\alpha)^{-1/3}-1])$	$(1-2\alpha/3)-(1-\alpha)^{2/3}$
Power law	Pz	$z\alpha^{[1-1/z]}$	$\alpha^{1/z}$
Prout-Tomkins	PT	$\alpha(1-\alpha)$	$\ln(\alpha/1-\alpha)$

[a] $n = 1/2$ corresponds to phase boundary controlled reaction (contracting area) and $n = 2/3$ corresponds to phase boundary controlled reaction (contracting volume).
[b] $m = 1,2,3$ or 4 when the growth rate of nuclei is proportional to the interphase area and can be 0.5; 1.5 or 2.5 in some cases of diffusion controlled growth rate of nuclei.

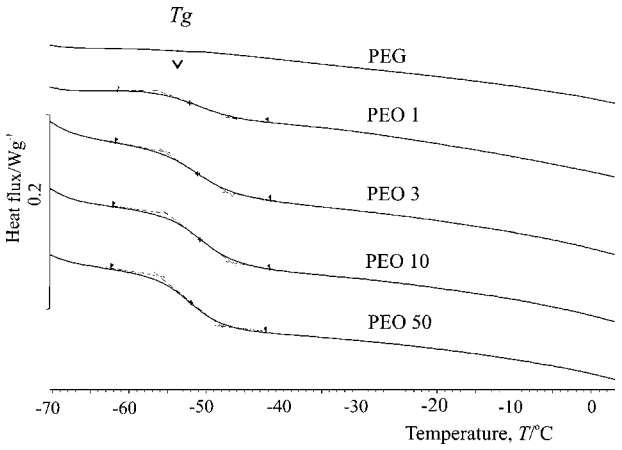

Fig. 1. The normalized DSC curves of PEG and PEOs; glass transition temperatures.

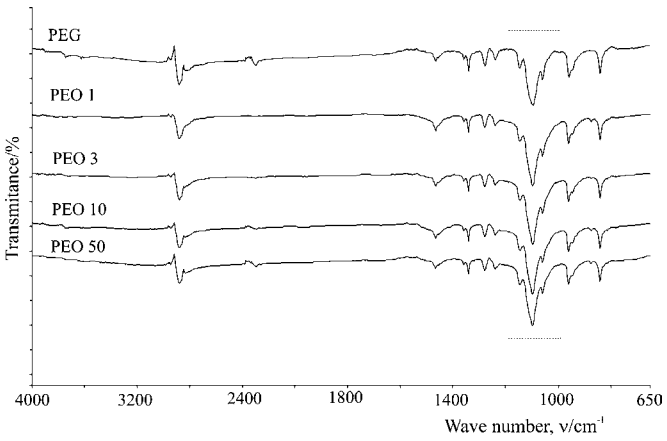

Fig. 4. The FT-IR spectra of PEG and PEOs.

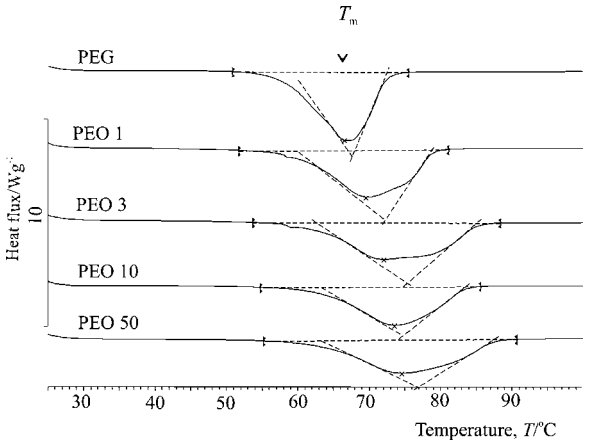

Fig. 2. The normalized DSC curves of PEG and PEOs; endotherms.

3.1. Isoconversional methods

Isoconversional methods enable determination of E directly from experimental α–T data ($\alpha = (m_0 - m)/(m_0 - m_f)$, where m_0, m and m_f refer to the initial, actual and residual mass of the sample) obtained at several heating rates without the knowledge of $f(\alpha)$. Isoconversional Flynn–Wall–Ozawa (FWO), Kissinger–Akahira–Sunose (KAS)) and Friedman (FR) methods have been used.

FWO method is a linear integral method based on Eq. (2):

$$\log \beta = \log \frac{AE_{iso}}{Rg(\alpha)} - 2.315 - 0.4567\frac{E_{iso}}{RT} \quad (2)$$

KAS is a linear integral method based on Eq. (3):

$$\ln \frac{\beta}{T^2} = \ln \frac{AR}{Eg(\alpha)} - \frac{E_{iso}}{RT} \quad (3)$$

FR method is a linear differential method based on Eq. (4):

$$\ln \left[\beta \frac{d\alpha}{dT}\right] = \ln A + \ln f(\alpha) - \frac{E_{iso}}{RT} \quad (4)$$

The plots $\log \beta$ vs. $1/T$, $\ln(\beta/T^2)$ vs. $1/T$ and $\ln[\beta\, d\alpha/dT]$ vs. $1/T$ obtained for α = const. from α–T curves recorded at several heating rates should be straight lines whose slopes allow calculation of E_{iso} by means of FWO, KAS and FR method, respectively.

3.2. Invariant kinetic parameters (IKP) method

IKP method also requires several α–T curves recorded at different heating rates and can be used only if the E does not depend on α, what must be previously checked by isoconversional methods. IKP method gives values of the invariant kinetic parameters, E_{inv} and A_{inv}, which correspond to the true kinetic model that describes the investigated process at all heating rates [18]. It is based on the existence of the linear compensation effect (Eq. (5)) between E and $\ln A$ obtained for the same TG curve by various theoretical kinetic

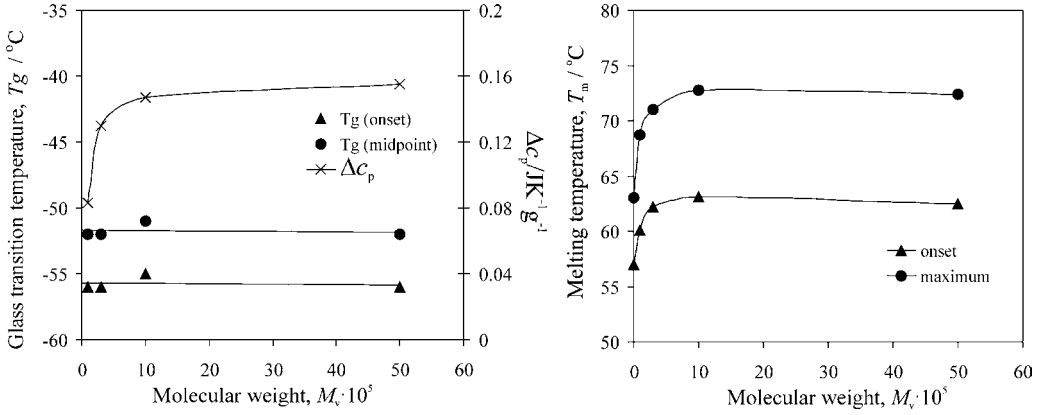

Fig. 3. The dependence of DSC curves characteristics of PEG and PEOs on molecular weight.

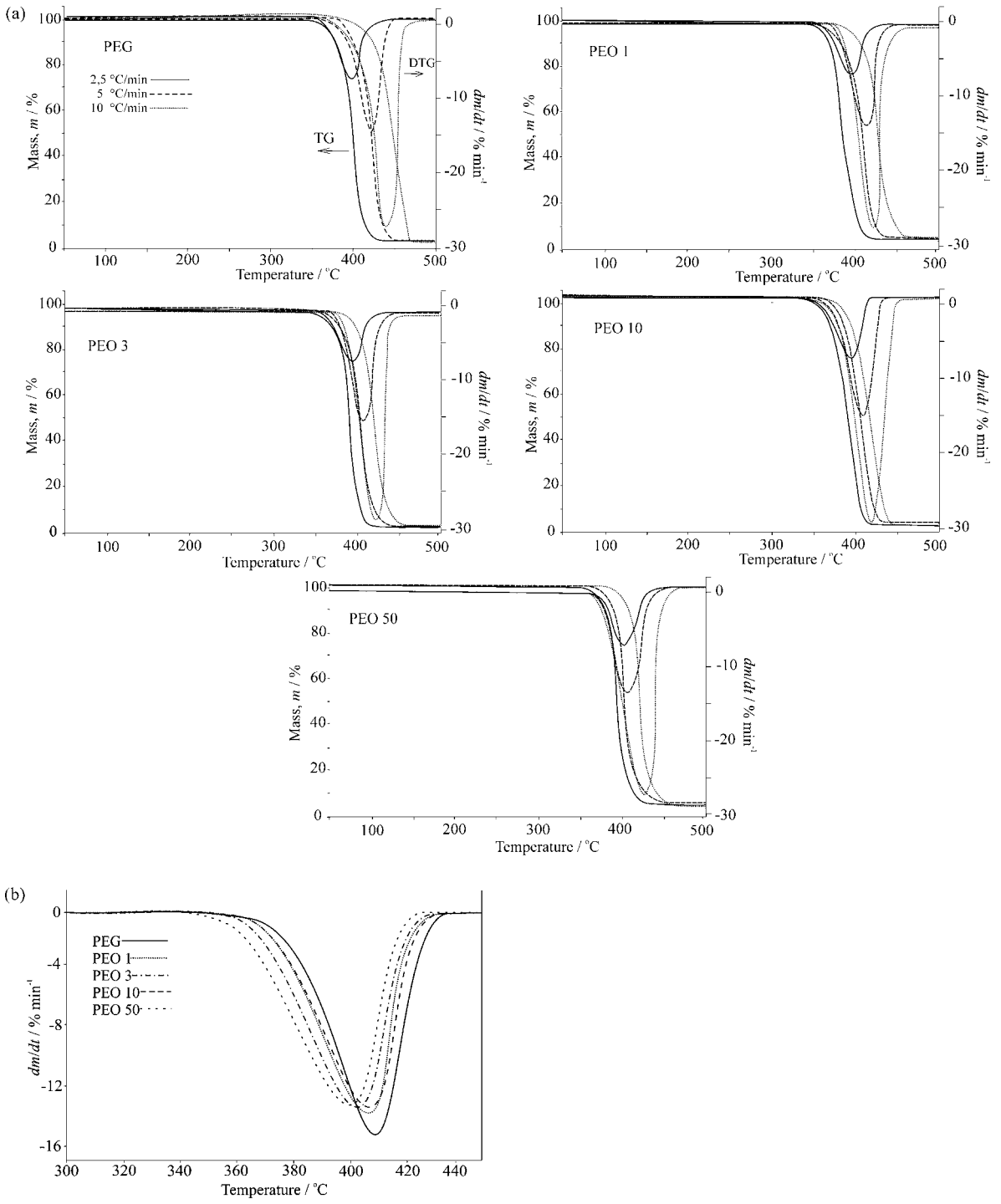

Fig. 5. (a) TG and DTG curves of dynamic thermal degradation of PEG and PEOs. (b) DTG curves of dynamic thermal degradation of PEG and PEOs at the heating rate of 5 °C min^{-1}.

models:

$$\ln A = a^* + b^* E \tag{5}$$

where a^* and b^* are the compensation effect parameters.

These values of E and $\ln A$ are obtained from the slope and intercept of plots $\ln[g(\alpha)/T^2]$ vs. $1/T$ by using model-fitting Coats-Redfern (CR) method [19] according to Eq. (6)

$$\ln \frac{g(\alpha)}{T^2} \cong \ln \frac{AR}{\beta E} - \frac{E}{RT} \tag{6}$$

$$g(\alpha) = \int_0^\alpha \frac{1}{f(\alpha)} d\alpha \tag{7}$$

for each theoretical kinetic model, $g(\alpha)$, and each heating rate, β. Algebraic expressions for the most frequently used mechanisms are shown in Table 1.

If the compensation effect exists, the straight lines $\ln A$ vs. E should be obtained for each heating rate and should intersect in a point that corresponds to the true values of E and $\ln A$ for the true kinetic model, which are called the invariant kinetic param-

eters, E_{inv} and A_{inv} by Lesnikovich and Levchik [13]. Due to the fact that certain variations of the experimental condition determine region of intersection, the intersection is only approximate. Therefore, in order to eliminate the influence of experimental conditions on determination of E_{inv} and A_{inv}, they are determined from the slope and intercept of the supercorellation relation (Eq. (8)):

$$a^* = \ln A_{inv} - b^* E_{inv} \quad (8)$$

Introducing E_{inv} and A_{inv} in Eq. (1) [20] gives numerical values of kinetic model, $f_{inv}(\alpha)$. The shape of experimental curves $f_{inv}(\alpha)$ vs. α suggests the algebraic expression of $f(\alpha)$ corresponding to analysed process. The correctness of kinetic analysis is checked by Pérez-Maqueda et al. criterion [14]. This criterion states that only in the case of true $f(\alpha)$ all experimental data (at all heating rates) lie on the single straight line $\ln[(d\alpha/dt)/f(\alpha)]$ vs. $1/T$ whose slope and intercept give the true values of the activation energy and pre-exponential factor. If the experimental results $\ln[(d\alpha/dt)/f(\alpha)]$ vs. $1/T$ are spread in separate lines for each heating rate, the considered $f(\alpha)$ does not fulfil the criterion, i.e. it is not capable to fit experimental results. Finally, if the correct kinetic triplets have been determined, E and E_{iso} values should be similar.

4. Results and discussion

4.1. Differential scanning calorimetry

The results of the DSC investigation of PEG and PEOs are shown as normalized DSC curves. The DSC heating curves show one glass transition temperature (T_g) at −56 °C (onset) or at −52 °C (midpoint) (Fig. 1) and one endotherm which represents the melting of the crystal phase of semi-crystalline polymer (Fig. 2). The exception is PEG for which determination of T_g is not possible. T_g of PEOs remains unchanged by increasing molecular weight while Δc_p increases, as well as the melting temperatures (T_m) of all investigated samples from 57 to 63 °C ($T_{m(onset)}$), or from 63 to 73 °C ($T_{m(max)}$), as shown in Fig. 3. Pielichowski and Flejtuch [22] have investigated the influence of the molecular weight of PEG (from 1000 to 35,000) on the melting and crystallization behaviour by means of DSC in dynamic mode at different heating rates. They have found an increased tendency of higher molecular weight PEGs towards the formation of crystalline phase owning to their lower segmental mobility and more convenient geometrical alignment and increase in T_m with increase of molecular weight.

4.2. Fourier transform-infra red spectroscopy

FT-IR spectra of the PEG and PEOs are presented in Fig. 4. Characteristic absorption bands have been identified as follows: C–O, C–C stretching, CH_2 rocking at 840 cm^{-1}, CH_2 rocking, CH_2 twisting at 960 cm^{-1}, C–O, C–C stretching, CH_2 rocking at 1058 cm^{-1}, C–O, C–C stretching at 1097 cm^{-1}, C–O stretching, CH_2 rocking at 1145 cm^{-1}, CH_2 twisting at 1241 and 1278 cm^{-1}, CH_2 wagging at 1341 cm^{-1} and CH_2 scissoring at 1466 cm^{-1}. There is no difference in FTIR spectra of PEG and PEOs due to their different molecular weights. The presence of the triplet peak of the C–C, C–O stretching vibration in the region of wave numbers from 1000 to 1200 cm^{-1} is the evidence of existence of crystalline phase and it was found in all spectra. Pielichowski and Flejtuch [2] have investigated thermal degradation of PEO (M_w = 13,060) by coupled techniques TG/FT-IR and TG/MS and have found out that main degradation products are ethyl alcohol, methyl alcohol, alkenes, non-cyclic ethers, formaldehyde, acetic aldehyde, ethylene oxide, water, CO and CO_2.

Table 2
Dependence of the thermal degradation characteristics of PEG and PEOs on M_v.

Sample	$M_v \cdot 10^{-5}$	$T_{5\%}$ (°C)	T_{max} (°C)	R_{max} (% min^{-1})	α_{max}	m_f (%)
Heating rate, β = 2.5 °C min^{-1}						
PEG	0.034	358	386	7.58	0.66	1.4
PEO 1	1	355	393	7.51	0.65	4.4
PEO 3	3	358	393	7.28	0.64	3.9
PEO 10	10	356	392	7.06	0.63	3.5
PEO 50	50	359	395	7.45	0.65	4.4
Heating rate, β = 5 °C min^{-1}						
PEG	0.034	374	410	15.0	0.62	1.1
PEO 1	1	369	406	14.2	0.63	4.4
PEO 3	3	369	405	13.7	0.64	3.9
PEO 10	10	372	408	13.9	0.64	4.3
PEO 50	50	364	403	13.5	0.65	3.9
Heating rate, β = 10 °C min^{-1}						
PEG	0.034	391	426	27.4	0.60	1.9
PEO 1	1	383	419	28.9	0.57	4.3
PEO 3	3	383	419	27.5	0.58	3.5
PEO 10	10	381	417	26.2	0.59	3.6
PEO 50	50	378	418	28.0	0.63	3.3

4.3. Dynamic thermogravimetry

The results of dynamic thermal degradation of PEG and PEOs in the thermobalance are thermogravimetric (TG) (mass loss vs. temperature) and derivative thermogravimetric (DTG) curves (mass loss rate vs. temperature) shown in Fig. 5(a) and (b). From TG and DTG curves it is evident that thermal degradation of investigated polymers occurs through one degradation step in temperature region from 330 to 450 °C. TG curves move towards higher temperatures by increasing the heating rate.

The characteristics of TG and DTG curves, $T_{5\%}$, T_{max}, R_{max}, α_{max} and m_f (Table 2) depend on the heating rate. The thermal stability, represented as $T_{5\%}$, does not significantly change with molecular weight. The maximal degradation rate (R_{max}) for PEG and PEOs occurs at T_{max} = 386 and T_{max} = 393 ± 1 °C, respectively, while T_{max} for PEG was 8 °C higher than for PEOs at the heating rate 10 °C min^{-1}. Obviously, the heating rate influences the degradation rate of investigated polymers in a different manner. R_{max} was achieved at conversion of around 60% for all investigated samples and heating rates. The final mass losses of approximately 1.5% for PEG and 4.0% for PEOs are independent of molecular weight and heating rate.

4.4. Kinetic analysis

Kinetic analysis is presented on a sample PEO 1, while the results for other samples are given in corresponding tables and figures. Firstly, the dependence of E_{iso} on α is established using isoconversional methods. For each selected α = const., the corresponding plots according to Eqs. (2)–(4) are obtained and from their slopes values of E_{iso} are calculated, respectively. The dependences of E_{iso} on α evaluated by means of FWO (a), KAS (b) and FR (c) method are shown in Fig. 6(a)–(c), respectively.

It is concluded from Fig. 6 that E_{iso} is practically independent on α in a conversion range from $0.04 \leq \alpha \leq 0.94$ for all investigated samples. This means that from the kinetical point of view investigated process is simple (one-step process) and can be described by unique kinetic triplet. This is in an agreement with investigation of Madorsky and Strauss [23] who have established that PEO decomposes in a single-stage by random scission of the chain links without chain-end-initiaded depolymerization. The average E_{iso} values in the conversion range $0.04 \leq \alpha \leq 0.94$ are shown in Table 3.

Kinetic data obtained at very high α values (here over 0.94) are not reliable due to deviation of actual temperature from preset one that may invalidate any evaluation of kinetic parameters [24].

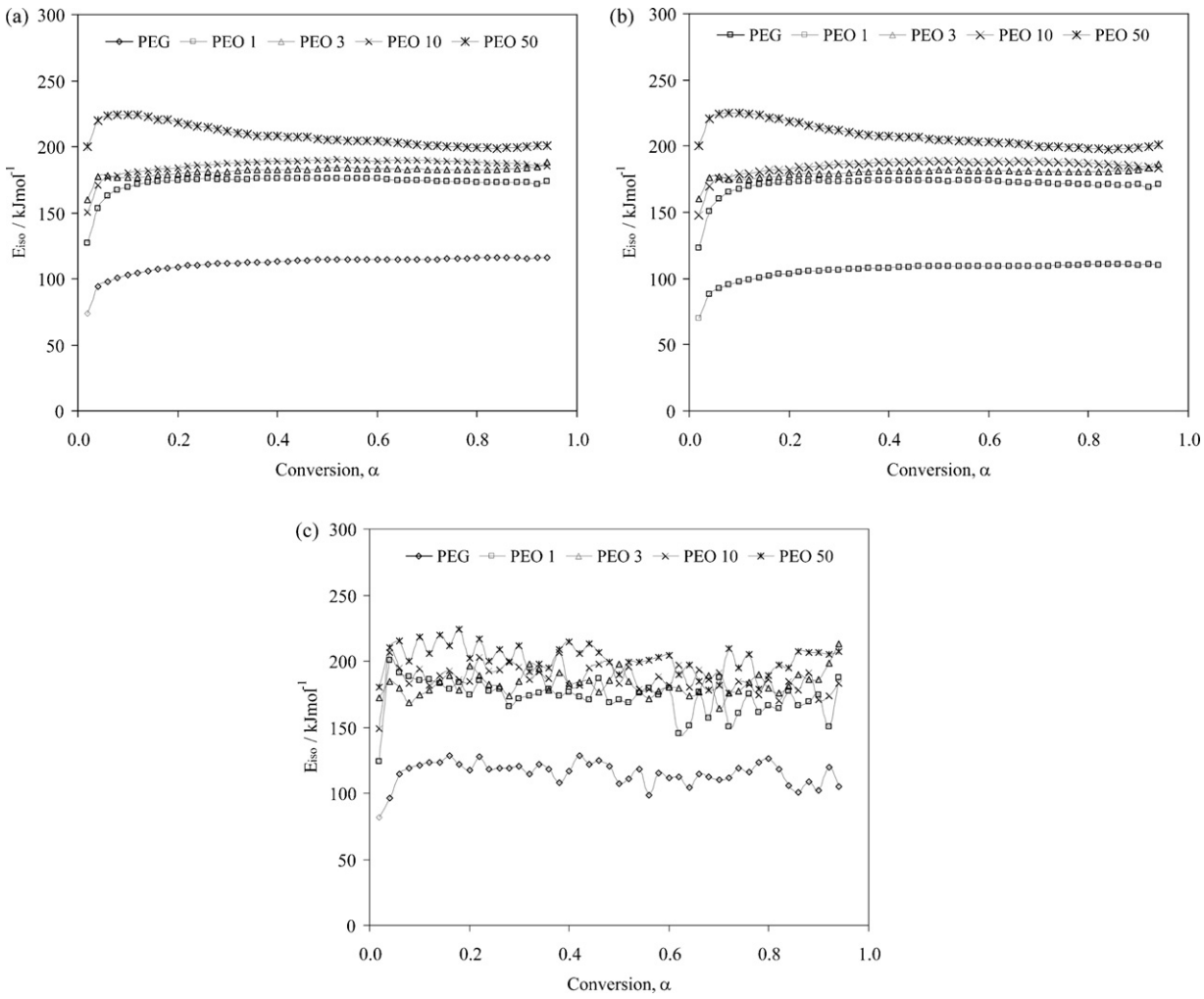

Fig. 6. The dependence of E_{iso} on α evaluated by means of FWO (a), KAS (b) and FR (c) method for the non-isothermal degradation of PEG and PEOs.

Since E does not depend on α, IKP method can be used for evaluation of true kinetic triplet. E and $\ln A$ values needed for IKP method were evaluated by CR method. By using Eq. (5) the existence of the compensation effect between values of E and $\ln A$ obtained by CR method is checked. Fig. 7(a) shows the compensation relationship for the non-isothermal degradation of PEO 1.

From the slopes and intercepts the so-called compensation parameters a^* and b^* are obtained for each heating rate. Only values of E and $\ln A$ from $g(\alpha)$ that show correlation coefficient $r^2 > 0.99$ at all heating rates have been used for calculation of a^* and b^*. Furthermore, these lines intersect in a very small region (Fig. 7(b)) what indicates that the non-isothermal degradation of PEO 1 really is one-step process. Intersection of these lines depends on experimental conditions, so the calculation of the invariant kinetic parameters, E_{inv} and A_{inv} is performed using the supercorrelation relation (Eq. (8)). Fig. 8 shows that between compensation parameters a^* and b^* supercorrelation relation really exists and from the slope and intercept of the straight lines E_{inv} and A_{inv} are obtained, respectively. In the same way, for all other investigated samples the existence of the compensation effect between E and $\ln A$ and one-step process are confirmed. Calculated values of E_{inv} and A_{inv} for all samples are shown in Table 4.

The values of E_{inv} are in a good agreement with E_{iso} values obtained by isoconversional, especially by Friedman method (see

Table 3
The average E_{iso} values obtained by FWO, KAS and FR methods for PEG and PEOs.

Sample	PEG	PEO 1	PEO 3	PEO 10	PEO 50
Conversion range	$0.04 \le \alpha \le 0.94$[a]	$0.04 \le \alpha \le 0.94$[a]	$0.04 \le \alpha \le 0.94$[a]	$0.04 \le \alpha \le 0.94$[a]	$0.04 \le \alpha \le 0.94$[a]
FWO					
E_{iso} (kJ mol^{-1})	112.9 ± 3.3	175.6 ± 1.4	181.9 ± 1.8	187.6 ± 2.6	207.5 ± 7.6
r^2	0.98550	0.99996	0.99189	0.98636	0.97501
KAS					
E_{iso} (kJ mol^{-1})	107.6 ± 3.3	172.5 ± 1.5	180.1 ± 1.8	186.3 ± 2.6	207.1 ± 8.2
r^2	0.98215	0.99995	0.99066	0.98433	0.97894
FR					
E_{iso} (kJ mol^{-1})	116.2 ± 7.6	172.7 ± 10.0	182.4 ± 7.6	187.7 ± 8.5	204.0 ± 16.1
r^2	0.98856	0.99770	0.98937	0.99078	0.98355

[a] Conversion, α.

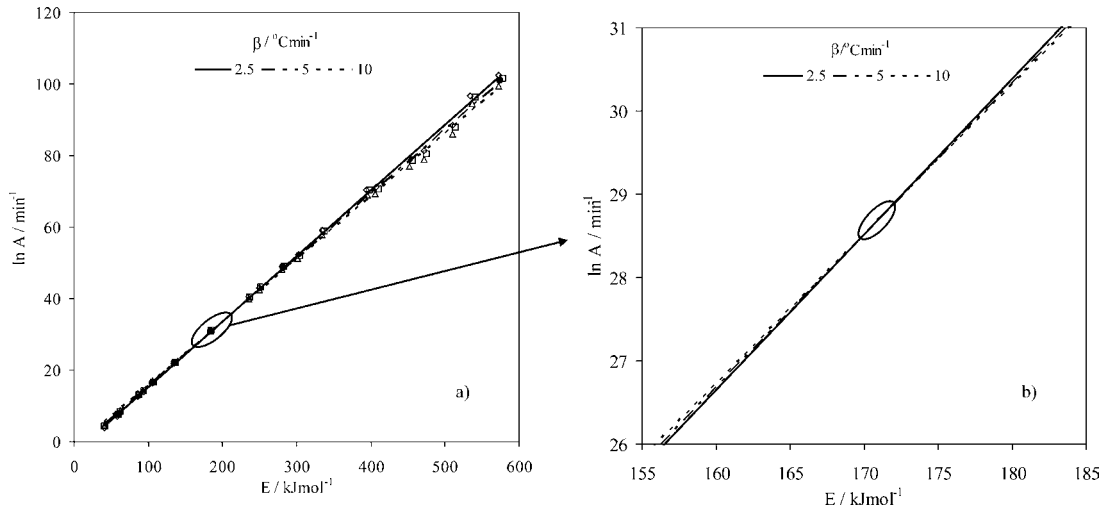

Fig. 7. The compensation relationship (a) and enlarged region of interception (b) for PEO 1.

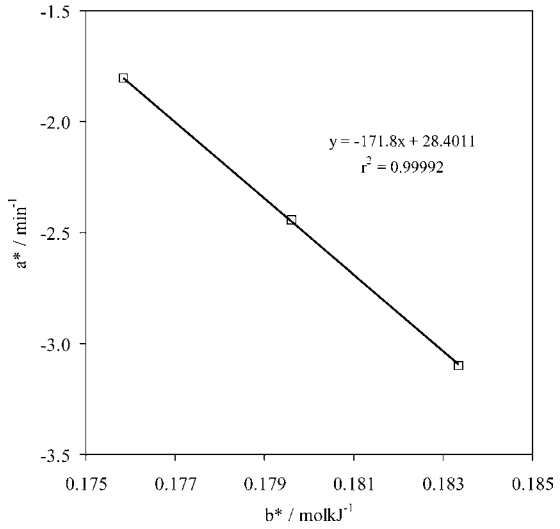

Fig. 8. The supercorrelation relationship for PEO 1.

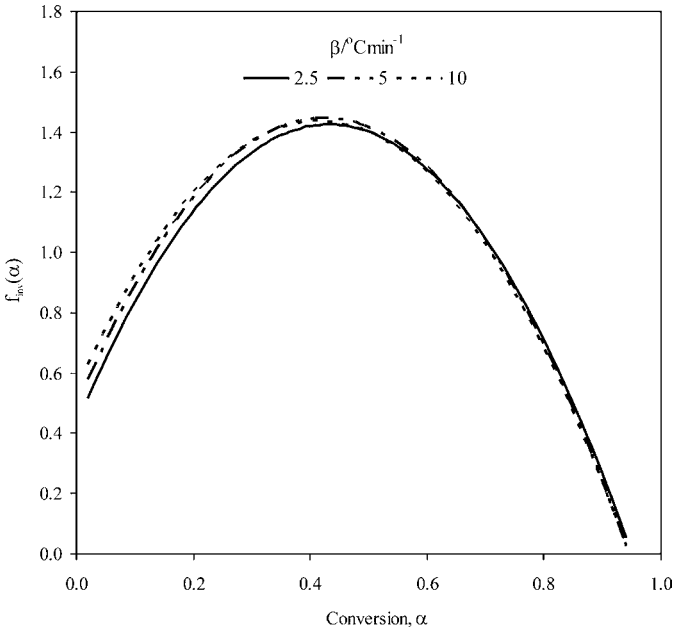

Fig. 9. The experimental dependence of $f_{inv}(\alpha)$ vs. α for PEO 1.

Table 3). Similar behaviour has already been observed for other polymers and polymeric materials [15,18,25]. Values of E_{inv} and A_{inv} allow numerical determination of $f_{inv}(\alpha)$ by introducing them into Eq. (1). Fig. 9 shows $f_{inv}(\alpha)$ vs. α curves for PEO 1. The curves exhibit the maximum as well as for all other samples considered in this work.

These curves are compared with the curves $f(\alpha)$ vs. α of the theoretical kinetic models (Table 1). Only Avrami–Erofeev kinetic models and Prout–Tomkins (PT) autocatalytic model exhibit maximum. It is well known that the true kinetic model should give E value similar to those obtained by isoconversional methods. PT model gives average E of 657 kJ mol^{-1} value in the conversion range $0.50 \leq \alpha \leq 0.94$ (up to $\alpha = 0.50$ CR method can not use PT model). Avrami–Erofeev A1.5 model gives average E value of 184 kJ mol^{-1} for PEO 1, the closest to isoconversional ones. This suggests that the non-isothermal degradation of PEO 1 occurs through mechanism like those represented by the Avrami–Erofeev equations. However, as expected, any theoretical Avrami–Erofeev kinetic model (Eq. (9)) cannot fit exactly the experimental $f_{inv}(\alpha)$ vs. α curve:

$$f(\alpha) = m(1-\alpha)[-\ln(1-\alpha)]^p \quad (9)$$

Therefore, it was necessary to calculate the empirical kinetic models that will fit exactly the experimental $f_{inv}(\alpha)$ vs. α curve, i.e. to calculate empirical parameters m and p for those models. The

Table 4
Values of invariant kinetic parameters for PEG and PEOs.

Sample	PEG	PEO 1	PEO 3	PEO 10	PEO 50
Conversion range	$0.04 \leq \alpha \leq 0.94$[a]	$0.04 \leq \alpha \leq 0.94$[a]	$0.04 \leq \alpha \leq 0.94$[a]	$0.04 \leq \alpha \leq 0.94$[a]	$0.04 \leq \alpha \leq 0.94$[a]
E_{inv} (kJ mol^{-1})	115.6	171.8	181.7	187.3	203.9
$\ln A_{inv}$ (min^{-1})	28.4	28.4	30.2	31.2	34.2
r^2	0.99992	0.99992	0.99267	0.99285	0.99999

[a] Conversion, α.

Table 5
The parameters m and p of empirical kinetic models for PEG and PEOs.

β (°C min^{-1})	PEG			PEO 1			PEO 3			PEO 10			PEO 50		
	m	p	r^2	m	p	r^2	m	p	r^2	m	p	r^2	m	p	r^2
2.5	3.29	0.65	0.98508	2.66	0.42	0.97676	2.44	0.33	0.97557	2.53	0.29	0.97625	2.48	0.31	0.97279
5	2.97	0.64	0.99128	2.63	0.38	0.97533	2.68	0.30	0.98199	2.32	0.30	0.97107	2.35	0.29	0.97415
10	3.27	0.58	0.99205	2.59	0.36	0.97279	2.45	0.31	0.97902	2.53	0.26	0.97101	2.33	0.22	0.99101
AV[a]	3.18	0.62	0.98947	2.63	0.38	0.97467	2.52	0.32	0.97886	2.46	0.28	0.97277	2.39	0.25	0.97932

[a] Average values of the parameters m and p.

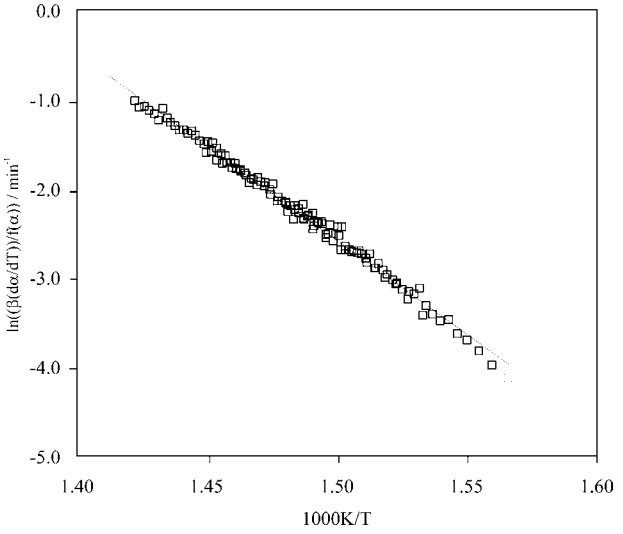

Fig. 10. Pérez-Maqueda et al. criterion applied on the empirical kinetic model for PEO 1.

parameters m and p are calculated for each heating rate from the intercepts and slopes of plots Y vs. ln[−ln(1 − α)] (Eq. (10)):

$$Y \equiv \ln \frac{d\alpha/dt}{1-\alpha} - \ln A_{\text{inv}} + \frac{E_{\text{inv}}}{RT} = \ln m + (-\ln(1-\alpha)) \tag{10}$$

obtained by introducing Eq. (9) into Eq. (1). If $p = 1 - 1/m$, then empirical $f(\alpha)$ corresponds to the theoretical Avrami–Erofeev kinetic model. Values of the parameters m and p of empirical kinetic models for PEG and PEOs are shown in Table 5.

The criterion by Pérez-Maqueda et al. was applied on the calculated empirical kinetic models (average values were considered). This criterion states that only in the case of true kinetic model all experimental results, at all heating rates, lay on the single straight line whose slope and intercept give the true values of the E and ln A (Fig. 10). It is evident that calculated empirical kinetic models fulfil this criterion for all investigated samples ($r^2 \approx 0.99$, Table 6) and from their slopes and intercepts the true values of E and ln A are obtained (Table 6). These E values are in a very good agreement with E_{iso} values. Theoretical kinetic models from Table 1 do not fulfil Pérez-Maqueda et al. criterion since the calculated data are spread in different lines.

The goodness of fit for each theoretical and empirical kinetic model in the conversion range $0.04 \leq \alpha \leq 0.94$ was estimated by

Table 7
Results of F-test for theoretical end empirical kinetic models.

$f(\alpha)$	F_j[a], Sample				
	PEG	PEO 1	PEO 3	PEO 10	PEO 50
EKM[b]	1.00	1.00	1.00	1.00	1.00
A0.5	1.45	1.57	1.70	1.66	1.31
A1 = F1	1.26	1.22	1.20	1.13	1.47
A1.5	1.62	1.41	1.21	1.26	2.12
A2	3.73	1.87	1.43	1.68	3.13
A2.5	3.20	2.55	1.80	2.34	4.49
A3	4.38	3.43	2.31	4.42	6.20
A4	7.48	5.79	3.74	5.61	10.65
R2	4.67	3.20	2.18	3.06	5.87
R3	54.17	34.70	140.48	32.80	62.52
F2	185.76	144.09	101.61	150.51	190.16
F3	68.30	55.36	40.47	58.65	68.02
D1	12.99	11.89	9.67	13.04	11.86
D2	40.12	33.52	25.16	37.32	39.13
D3	40.97	14.89	11.37	15.78	16.72
D4	7.77	7.13	5.80	7.62	7.13
P2	76.26	58.01	40.72	59.54	75.68
P3	59.30	45.15	31.71	46.06	57.83
P4	49.11	37.59	26.35	67.77	48.10

[a] $F_{1-p,n-1,n-1} = 1.69$; $n = 41$; $p = 0.05$.
[b] EKM = empirical kinetic model.

using the residual sum of squares (Eq. (11)):

$$S_j^2 = \frac{1}{n-1}\sum_{i=1}^{n}\left(\left(\frac{d\alpha}{dt}\right)_{\text{exp}} - \left(\frac{d\alpha}{dt}\right)_{\text{model}}\right)^2 \tag{11}$$

where n is the number of data points (in our case $n = 41$), $(d\alpha/dt)_{\text{exp}}$ the experimental and $(d\alpha/dt)_{\text{model}}$ the calculated values, respectively. Since the minimum value of S^2 does not necessarily indicate "the most probable" kinetic model, we have performed the so-called F-test (Eq. (12)):

$$F_j = \frac{S_j^2}{S_{\text{min}}^2} > F_{1-p,n-1,n-1} \tag{12}$$

where S_{min}^2 is the minimum value of all S_j^2 and $F_{1-p,n-1,n-1}$ is a percentile of the F-distribution for $(1-p)100\%$ confidence probability. According to F-test, only those reaction models which obey Eq. (12) should be discriminated as giving S_j^2 that are significantly larger than S_{min}^2 and therefore not belonging to the set of "the best fit" models. The reaction models which obeyed Eq. (12) fit experimental data as accurately as the model that gives S_{min}^2 [26]. F_j values in Table 7 show that from the point of view of F-test the empirical

Table 6
Values of E and ln A corresponding to empirical kinetic models for PEG and PEOs.

Sample	Conversion, α	$f(\alpha)$	E (kJ mol^{-1})	ln A (min^{-1})	r^2
PEG	$0.04 \leq \alpha \leq 0.94$	$3.18(1-\alpha)[-\ln(1-\alpha)]^{0.62}$	116.9	18.6	0.98641
PEO 1	$0.10 \leq \alpha \leq 0.90$	$2.63(1-\alpha)[-\ln(1-\alpha)]^{0.38}$	172.9	28.5	0.99074
PEO 3	$0.10 \leq \alpha \leq 0.90$	$2.52(1-\alpha)[-\ln(1-\alpha)]^{0.32}$	181.4	30.1	0.98863
PEO 10	$0.10 \leq \alpha \leq 0.90$	$2.46(1-\alpha)[-\ln(1-\alpha)]^{0.28}$	188.0	31.3	0.98976
PEO 50	$0.10 \leq \alpha \leq 0.90$	$2.39(1-\alpha)[-\ln(1-\alpha)]^{0.25}$	201.4	33.7	0.99404

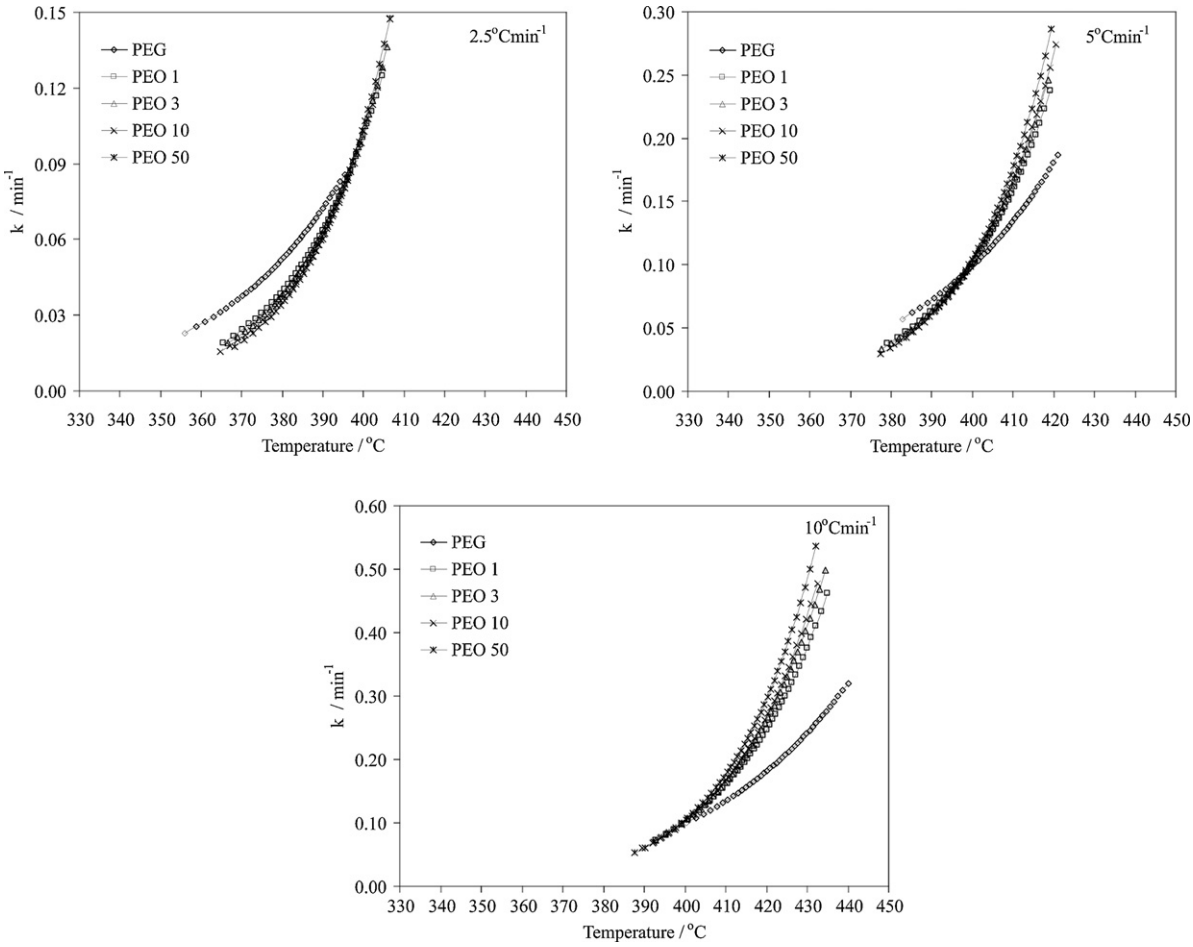

Fig. 11. Dependence of k on T for PEG and PEOs.

and theoretical Avrami–Erofeev kinetic models are "the most probable" ones (A0.5, A1 and A1.5 for PEG and PEO 1; A1, A1.5 and A2 for PEO 3; A0.5, A1, A1.5 and A2 for PEO 10; A0.5 and A1 for PEO 50).

The corresponding E and $\ln A$ values for these "the most probable" theoretical kinetic models calculated using CR method are shown in Table 8. Since these E values significantly differ from E_{iso} values (except E value corresponding to A1.5 for PEO 3), it is our opinion that empirical kinetic models are the best description of the investigated process.

Table 8
E and $\ln A$ values for "the most probable" theoretical kinetic models.

Sample	Kinetic model	E (kJ mol^{-1})	$\ln(A/\text{min}^{-1})$	r^2
PEG	A0.5	590.7	103.1	0.99941
	A1	289.7	50.2	0.99939
	A1.5	189.3	32.0	0.99949
PEO 1	A0.5	574.1	101.2	0.99951
	A1	281.5	48.7	0.99948
	A1.5	183.9	31.1	0.99946
PEO 3	A1	277.8	48.1	0.99902
	A1.5	181.4	30.6	0.99897
	A2	133.3	31.8	0.99989
PEO 10	A0.5	560.2	98.8	0.99929
	A1	274.5	47.5	0.99926
	A1.5	179.3	30.3	0.99922
	A2	131.7	21.5	0.99918
PEO 50	A0.5	551.8	97.3	0.99975
	A1	270.3	46.8	0.99974

Finally, the true values of E and $\ln A$ allow calculation of the rate constant, k ($k = A \cdot \exp(-E/RT)$) for the non-isothermal degradation of PEG and PEOs (Fig. 11).

At the lower heating rate (2.5 °C min^{-1}) samples with higher molecular weight show lower k values than those with lower molecular weight. The results reverse with the increase of the heating rate, so at the heating rate of 10 °C min^{-1} samples with higher molecular weight show higher k values compared to samples with lower molecular weight. This is in accordance with results obtained from TG and DTG curves (Table 2).

5. Conclusions

DSC and FT-IR spectroscopy show that all investigated samples are semi-crystalline polymers. The glass transition temperatures of PEOs are independent of their molecular weight while the change of specific heat capacity in glass transition increases with molecular weight. The melting temperatures of PEG and PEOs shift towards higher temperatures by increasing molecular weight. The thermal degradation of those polymers investigated by dynamic TG shows that PEG and PEOs degrade in one degradation step in temperature region from 330 to 450 °C. According to characteristics of TG and DTG curves it could be concluded that thermal degradation of PEG and PEOs occurs in the same temperature region almost independently of molecular weight. The empirical kinetic triplets for the non-isothermal degradation of PEG and PEOs were calculated by combined use of isoconversional Flynn–Wall–Ozawa, Kissinger–Akahira–Sunose and Friedman methods and invariant kinetic parameters method associated with the criterion of the

independence of kinetic triplet on the heating rates. It was found that samples with higher molecular weight degrade slower at the lower heating rates, while at higher heating rates samples with higher molecular weight degrade faster than those with lower molecular weight.

Acknowledgement

This work is financially supported by the Ministry of Science, Education and Sports of the Republic of Croatia (scientific project "Polymer blends with biodegradable components").

References

[1] J. Kahovec, R.B. Fox, K. Hatada, Pure Appl. Chem. 74 (2002) 1921–1956.
[2] K. Pielichowski, K. Flejtuch, J. Anal. Appl. Pyrol. 73 (2005) 131–138.
[3] M.M. Crowley, F. Zhang, J.J. Koleng, J.W. McGinity, Biomaterials 23 (2002) 4241–4248.
[4] F.Y. Wang, C.C.M. Ma, W.J. Wu, J. Appl. Polym. Sci. 80 (2001) 188–196.
[5] T. Ozawa, Bull. Chem. Soc. Jpn. 38 (1965) 1881–1889.
[6] J.H. Flynn, L.A. Wall, J. Res. Natl. Bur. Stand. 70A (1966) 487–523.
[7] R. Audebert, C. Aubineau, Eur. Polym. J. 6 (1970) 965–979.
[8] E. Calahorra, M. Cortezar, G.M. Guzman, J. Polym. Sci. Lett. Ed. 23 (1985) 257–260.
[9] F. Barbadillo, J.L. Mier, R. Artiaga, R. Losada, L. García, Proceedings of the eight European Symposium on Thermal Analysis and Calorimetry, Barcelona, 2002, p. 75.
[10] H.E. Kissinger, Anal. Chem. 29 (1957) 1702–1706.
[11] T. Akahira, T. Sunose, Res. Rep. Chiba Inst. Technol. 16 (1971) 22–31.
[12] H.L. Friedman, J. Polym. Sci. 6C (1963) 183–195.
[13] A.I. Lesnikovich, S.V. Levchik, J. Therm. Anal. 27 (1983) 89–94.
[14] L.A. Pérez-Maqueda, J.M. Criado, F.J. Gotor, J. Malek, J. Phys. Chem. A 106 (2002) 2862–2868.
[15] P. Budrugeac, Polym. Degrad. Stab. 89 (2005) 265–273.
[16] S. Vyazovkin, A.I. Lesnikovich, Thermochim. Acta 165 (1990) 273–280.
[17] S. Vyazovkin, N. Sbirrazzuoli, Macromol. Rapid Commun. 27 (2006) 1515–1532.
[18] P. Budrugeac, E. Segal, Int. J. Chem. Kin. 33 (2001) 564–573.
[19] A.W. Coats, J.P. Redfern, Nature 201 (1964) 68–69.
[20] P. Budrugeac, E. Segal, L.A. Pérez-Maqueda, J.M. Criado, Polym. Degrad. Stab. 84 (2004) 311–320.
[21] K. Pielichowski, J. Njuguna, Thermal Degradation of Polymeric Materials, Rapra Technology Limited, Shawbury, 2005, p. 40.
[22] K. Pielichowski, K. Flejtuch, Polym. Adv. Technol. 13 (2002) 690–696.
[23] S.L. Madorsky, S. Strauss, J. Polym. Sci. 36 (1959) 183–194.
[24] M. Maciejewski, Thermochim. Acta 355 (2000) 145–154.
[25] M. Erceg, T. Kovačić, S. Perinović, Thermochim. Acta 476 (2008) 44–50.
[26] S. Vyazovkin, C.A. Wight, Thermochim. Acta 340–341 (1999) 53–68.